https://doi.org/10.1016/j.energy.2020.118433

A Novel Ramp-Rate Control of Grid-Tied PV-Battery Systems to Reduce Required Battery Capacity

Yujia Huo*, Giambattista Gruosso

Dipartimento di Elettronica Informazione e Bioingegneria, Politecnico di Milano
Piazza Leonardo da Vinci 32, 20133 Milan, Italy

Abstract

This paper proposes a novel ramp-rate control of PV-battery systems in microgrids. The nearby time-varying loads are innovatively included in the proposed control strategy. Within permissible operating range, the power consumed by the loads is regulated and participates in mitigating the overall ramp-rate of the controlled PV system and the loads. The control strategy is grid-friendly as the power fluctuation of the loads is also considered besides that of the PV system. Furthermore, this control strategy economizes on the auxiliary batteries of the PV system since a part of the required active power is now borrowed from the loads. The virtual synchronous generator technology is applied in this ramp-rate control to further reduce the use of the batteries and to provide ancillary service. Numerical simulations on a test microgrid indicate the effectiveness of the ramp-rate control. The test cases also demonstrate that this control strategy succeeds in reducing the battery capacity and the number of battery cycles as well as in offering frequency support to the microgrid.

Keywords: Battery Energy Storage System; Photovoltaics; Ramp-Rate Control; Virtual Synchronous Generator

1. Introduction

Solar energy is a promising clean energy resource in the near future. Together with other renewables, it produces a revolution in power system with plenty merits, but at the same time the increasing integration of PV systems challenges the power quality and stability of the grid [1, 2, 3, 4]. One concern is the high power ramp-rate (RR). It is commonly attributed to the intermittency of PV generation due to varying irradiance. Therefore, many countries have issued regulations to limit the RR of PV power. As described by National Renewable Energy Laboratory in [5], Puerto Rico Electric Power Authority and transmission system operators in Germany require a 10% of rated capacity limit on 1-minute RR by both wind and PV generation. With the purpose of mitigating the detriment to the grid, many RR control methods have been proposed. In most of them, energy storage systems (ESSs) have played an essential role [6].

Viable choices of storage technologies can be flywheel, supercapacitor, battery, etc. Performances of the storage technologies in RR control have been investigated in [7]. Among them, the battery is the most common option due to high controllability and quick response [8, 9]. But on the other hand, batteries are sensitive to operating situations so they deteriorate as a result of undesired operation. Moreover, the uncertain (dis)charge process during the control makes the estimation of the battery capacity difficult and thereby leading to redundant assessment. Some works have investigated the ways to estimate the capacity, cost and aging of the battery in RR control [10, 11, 12, 13]. Nevertheless, the efficiency of the use of battery

*Corresponding author
Email address: yujia.huo@polimi.it (Yujia Huo)

depends on the definition of the control methods as well [14]. A few works have discussed about the self-curtailed method where PV systems conduct an under maximum power point tracking (MPPT) at a power ramp-up, thereby removing power from the detected curve for unidirectional RR compensation [15, 16, 17]. In this way, the battery energy storage system (BESS) only compensates the power ramp-down. One feature of this strategy is that the battery discharges during the day and gets charged slowly at night. Therefore, the initial state of charge (SoC) can be set to a high value bringing down the required capacity as well as the number of charge cycles. The work in [18] proposes a coordinate RR control strategy for PV subsystems, thereby restricting the overall output power RR of the whole PV plant. Theoretically, it is able to achieve storage-free given a sufficient number of irrelevant PV subsystems, but a BESS is still suggested in case of critical situations. In summary, RR control solutions today focus on not only the literal duty but also the efficient utilization of batteries. Reducing the capacity of the battery or eliminating the battery is favored under this topic. Since the use of batteries is almost unavoidable, the efficiency of utilization is another significant index of RR control strategies.

According to control goals, RR control methods can be classified into ramp-rate smoothing (RRS) and ramp-rate limiting (RRL) ones. RRS solutions aim to smooth the fluctuating power curve so the RR is the uncontrolled result of the action. RRL solutions, on the contrary, monitor the power curve to obtain the RR and involve the RR in the control schemes afterwards. The action can be either continuous along with the change of RR or triggered by pulses that signify the exceeding of the RR over a preset limit. The representative of RRS is the frequently used filter smoothing. BESSs generate or absorb active power according to the difference between the output power of PV and the filter smoothed power curve. The key to reduce unnecessary use of batteries is to minimize the phase shift of the fundamental power curve, because the phase shift at low frequency demands continuous power from BESSs even in uncritical situations. So the design principle of the filter is to optimize the trade-off between the attenuation of the spikes and the phase shift of the main curve. The minimum order under certain constraints is thus preferable. For finite impulse response (FIR) filters, Gaussian, Kaiser, Rectangular windows and moving average (MA) are sharp enough to this end and their performances are comparable. Infinite impulse response (IIR) filters, adding the manageability of poles, are more flexible to build dedicated pass and stop bands. With fixed order and coefficients, filtering methods do not control the RR to particular values. The change of weather is random, so the RR risks exceeding the boundary unless the worst case is used to design the filter and the BESS. However, the over-design causes superfluous RR smoothing and excessive use of BESS in normal operation. Therefore, advanced filter techniques are proposed to alleviate this issue. In [19], Kalman Filter is applied with the state of the battery being one factor of the control and in [14], exponential moving average (EMA) with dynamic parameter is employed to counter with the memory effect. Fuzzy control is utilized for smoothing the PV power with reduced requirement on batteries as described in [20, 21, 22]. However, like the conventional filter-based methods, they still do not regulate the RR directly either.

The second type of RR control is RRL whose goal is to keep the RR under a preset boundary. In contrast to RRS, RRL solutions eliminate the uncertainty over the resulted RR and normally utilize the BESSs more efficiently. There are many ways to design the control strategy according to the supervised variables. In [23, 24], the SoC of the battery is taken into consideration preventing forced shutdown of the BESS due to over-charge or over-discharge of the battery. In [25], a desired RR tracking method is proposed. It conducts tight RR control by means of the inverse characteristic of the desired RR until high RR disappears and then switches to a droop characteristic versus the SoC ensuring the availability of the BESS. In [26], a controlled dump load is installed in place of a BESS absorbing excessive power generated by the PV system under high RR. In this way, the PV system operates by MPPT so the control burden is transferred to the dump load side. The complexity of control and stability issues are less critical, but heat dissipation becomes another concern.

In the research on mitigating high RR, two technical points are worth attention. The first one is the definition of the control target. In previous literature, the power output of PV systems is controlled to meet a predefined RR standard. In a microgrid, however, high RR is not only due to intermittent renewable generation, but it is also affected by time-varying loads. In other words, quantifying the RR of a PV plant does not necessarily quantify the overall RR in a closely coupled area as the superposition effect is omitted. Certainly, it is obvious that monitoring and mitigating the RR of every power generator and consumer is

unfeasible, but changing the RR control target from a sole PV system to a set of neighboring PV systems and loads that couple at one point of common coupling (PCC) will undoubtedly reduce the uncertainty of the overall RR. The second technical point is the extent to which the RR control strategy relies on the BESS to meet the requirement. In low voltage systems, all RR control strategies share one intrinsic working principle that is to counteract the active power of high RR by another the other way round. But when it comes to specific design and implementation, they diverge from each other in composition of the system, definition of the control algorithms, available amount of power for regulation, final performance of the RR, control efficiency, cost, etc, and hence differences in the utilization of BESSs. Therefore, based on the premise that the RR can be limited according to the standard, ways to save on batteries can be:

(1) deployment of other active power sources to reduce or even to eliminate the utilization of batteries;
(2) efficient strategies to generate power reference for the BESS;
(3) smooth transition between control states;
(4) ...

Based on the aforementioned methodology, this paper proposes a novel RR mitigation strategy that incorporates the neighboring loads of the PV into the control system. The power consumption of the loads is regulated within the permissible range in order to counteract the overall high RR observed at the PCC, namely that a portion or all of the active power used for RR mitigation is supposed to be borrowed from the loads temporarily. This method will hereafter be called as *load compensation* for short. The control is performed inside the PV plant with a supervision at the PCC. For one thing, the automatic load compensation action can be triggered by the fluctuating power flow at the PCC and actuated by the PV power converters, and for another, the load operation ought to be monitored and controlled complying with the grid code. Since it is not planned to be a rigorous RR limiting method, the excessive power spikes are suppressed by the auxiliary BESS in grave situations. In gentle cases, the PV system can be even BESS-free. The anticipated merits of the proposed control are as follow:

(1) limitation of the overall RR at a PCC that joins more than one non-inertial component;
(2) reduction in the number of subsystems that contribute to the total RR;
(3) reduction in the reliance on BESS and improved lifespan of batteries thanks to the decreased (dis)charge cycles and depths.

In addition to load compensation, the situations in which the PV system performs as a virtual synchronous generator (VSG) are discussed as well based on the previous study on virtual inertia and damping [27]. The idea is to curtail the power output of the PV. The active power provided by the VSG substitutes for a portion or all of the active power required from the BESS. Unidirectional and bidirectional VSGs are presented to compare the use of batteries, the provision of ancillary service and the power loss.

A simplified microgrid is simulated to test the control strategy. The load compensation method proves effective in reducing the required battery capacity and in eliminating uncritical (dis)charge cycles. It also shows that the introduction of VSG can further cuts down the use of battery at the expense of power loss, providing information on the future optimization of cost and profit.

The paper is structured as follows. Section 2 expounds the working principle and the implementation of the proposed control strategy. Section 3 describes the test configuration and analyzes the test results. Finally, Section 4 presents the conclusions.

2. Proposed Ramp-Rate Limiting Method

The proposed RRL method will be elaborated in the context of a low-voltage weak microgrid. The configuration of the network and the block diagram of the control strategy are described in Figure 1. The PV plant with an auxiliary BESS (PV-BESS) and the loads are connected to the microgrid at the PCC. In order to clarify the working principle, the rest of the microgrid is approximated to a grid former functioning as active frequency and voltage control actuator.

In the proposed RR control method, the PV-BESS and its neighboring loads are seen as a unity joining to the microgrid at a PCC. Different from the aforementioned literature in which the PV system is studied

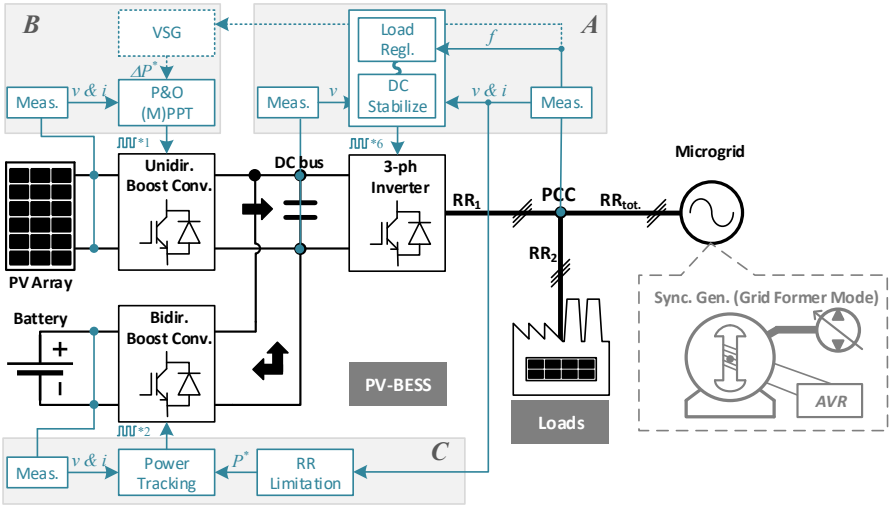

Figure 1: Configuration and control block diagram of the PV-BESS in microgrid.

alone, the proposed control strategy features the adjacent loads as a potential active power source for RR compensation and as a part of the RR control target. From grid operational perspective, the overall RR matters for the grid former, especially in weak microgrids. Therefore, gathering fragmented power profiles is supposed to indicate efficacious information. As it is shown in Figure 1, the total number of RR contributors is reduced from two to one. The unpredictable power perturbations come from ambient-condition-dependent renewable generation and choices of power purchasers. Figure 2 shows an example depicting the active power profiles accompanied by the RR of the PV system and that including the loads. The curves have indicated that the inclusion of loads makes the situation complex and severe.

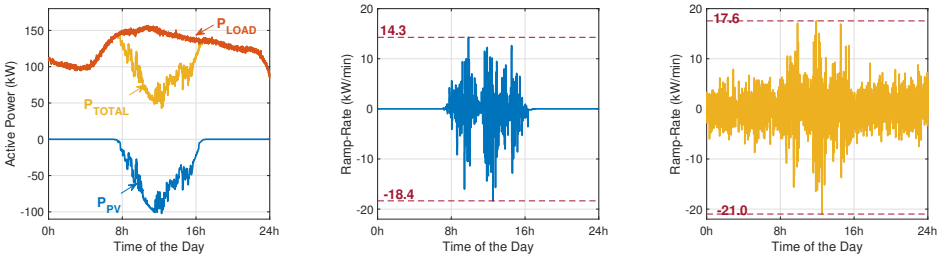

(a) Power curves of the load, the PV system and their summation

(b) Ramp-rate of the PV power

(c) Ramp-rate of the total power

Figure 2: Impact of the load on the overall ramp-rate.

The control strategy has been described briefly in Figure 1 based on a three-power-converter structure. The PV array and the battery join at the DC bus by a unidirectional boost converter and a bidirectional boost converter respectively and the PV-BESS is connected to the microgrid by a three phase inverter. Therefore, the control strategy is divided into three sections for the three power converters.

2.1. Control Section A

Control Section A controls the 3-phase inverter which interfaces the DC bus to the PCC. With the PCC voltage and current together with the DC bus voltage, it first stabilizes the DC bus. Then it automatically smooths the total active power curve by means of reactive power regulation.

Grid frequency is a symbol representing the evenness of the power curve endured by the grid former. It is set and maintained by the grid former mechanically with inertia (or electrically with virtual inertia). Because of the inertia, grid frequency has the reluctance to bear power changes but also to recover. Under frictionless assumption, the rotation motion of the rotor of a synchronous generator (SG) can be expressed as:

$$J\frac{d\omega}{dt} = T_m - T_e, \tag{1}$$

where ω is the electrical angular velocity; T_m is the mechanical torque and T_e is the electromagnetic torque applied to the rotor. T_e is related to the active power at the PCC, therefore, limiting RR is equivalent to removing the high frequency components of T_e. The goal equation then can be rewritten as:

$$J\frac{d\omega}{dt} = T_m - \frac{f_{smooth}(P_{total})}{\omega} = T_m - f_{smooth}(T_{total}), \tag{2}$$

where P_{total} is the total power of the loads and the PV-BESS joined at the PCC; T_{total} is the derived torque. We can infer that the total RR will be reflected on grid frequency and the rate of change of frequency. Based on the relationship between voltage, current, flux, electrical power and electromagnetic torque in machine theory, $f_{smooth}(T_{total})$ can be written as:

$$f_{smooth}(T_{total}) = \frac{3}{2}p({\phi_d}^r {i_q}^r - {\phi_q}^r {i_d}^r), \tag{3}$$

where p is the number of pole pairs; ϕ is the flux; i is the armature current. The d-q axis is defined according to the rotor position as indicated in the subscript (d or q component) and superscript (rotor based coordinate). Expressing the flux by current, Equation (3) can be further rewritten as:

$$f_{smooth}(T_{total}) = \frac{3}{2}p\big({L_{md}}^r i_f - \Delta {L_{mdq}}^r {i_d}^r\big){i_q}^r, \tag{4}$$

where i_f is the excitation current at the rotor side; L_m is the magnetizing inductance and $\Delta L_{mdq} = L_{md} - L_{mq}$. From Equation (4) we can know that, ${i_d}^r$ and ${i_q}^r$, which are determined by the PCC, are potential to smooth T_{total} caused by the ramping power. For round-pole SG, reducing ${i_q}^r$ rapidly can attenuate the ramp-up. For salient-pole SG, both reducing ${i_q}^r$ and increasing ${i_d}^r$ work for ramp-up. Since the smoothing operation is supposed to be implemented at the PCC instead of the rotor, the transformation of coordinate should be done in this way:

$$\begin{bmatrix} {i_d}^r \\ {i_q}^r \end{bmatrix} = \begin{bmatrix} sin\theta & -cos\theta \\ cos\theta & sin\theta \end{bmatrix} \begin{bmatrix} {i_d}^{PCC} \\ {i_q}^{PCC} \end{bmatrix}, \tag{5}$$

where θ is the torque angle and the superscript ^{PCC} represents the d-q coordinate set by the PCC voltage. If we leave the PV generation and the loads as they are, but make the PV-BESS absorb some reactive power after seeing power ramp-up, the change of rotor current will be:

$$\begin{cases} \Delta {i_d}^r = \frac{2}{3} \cdot cos\theta \cdot \frac{\Delta Q}{{v_d}^{PCC}} \\ \Delta {i_q}^r = -\frac{2}{3} \cdot sin\theta \cdot \frac{\Delta Q}{{v_d}^{PCC}} \end{cases}, \tag{6}$$

where ΔQ is the regulated reactive power and ${v_d}^{PCC}$ is the amplitude of the PCC voltage. The reactive power regulation at the PCC leads to a change of current that results in lowering down the power ramp-up. It works for ramp-down cases as well but the direction of the controlled reactive power should be in inverse.

In this way, the frequency stimulated reactive power control can realize load sharing within the united system of the PV and the loads. Not curtailing the output of the PV system, the power spikes due to the variation of irradiance will be compensated by the power change of the loads. This will transfer the power ramps to voltage ramps. According to the grid code, the voltage of the loads should not exceed a limit. In Italy for instance, ±10 % is defined by Terna as the maximum permissible voltage deviation.

Therefore, a voltage triggered saturation of the control is necessary. Load compensation is advantageous because the power curve will be smoothed just as it is done by the filter-based method, but achieved by power balancing among the non-inertial equipment internally, saving the estimated capacity of the battery. To shave excessive power spikes in severe cases, we can choose to apply power curtailment in the PV system to realize VSG or to regulate active power from the BESS, which will be discussed in Control Section B and C respectively.

The control is implemented as shown in Figure 3. The DC bus voltage is stabilized by controlling the active power in form of d-axis current in this case. The reactive power, which is related to the q-axis current, is linked with the frequency transient as grid frequency is an indicator of power ramps. The ideal reference for the q-axis current is designed to be proportional to frequency deviations that are out of the dead bind. But considering the permissible change of voltage at the PCC, a saturation must be applied when the PCC voltage goes out of the limit. Within the voltage limit, the reference for the q-axis current does not necessarily follow the ideal value all the time otherwise its discontinuity at desaturation will bring about power spikes. Therefore, a smooth transition between the saturated value and the ideal value must be inserted. In this case, the reference remains unchanged after desaturation until the ideal value becomes equal to the saturated value. The phase angle is defined by the PCC voltage and based on it, the voltage and current at the PCC are transformed into d-q coordinate. The inner current closed loop together with the forward control generates the voltage references. Knowing the measured DC bus voltage, the modulated waves are calculated and finally transformed back to three phase for pulse width modulation (PWM).

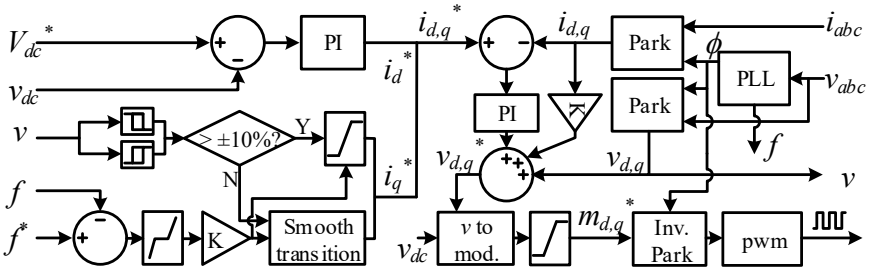

Figure 3: Implementation of Control Section A.

2.2. Control Section B

Control Section B controls the boost converter which connects the PV array to the three phase inverter. With the measured voltage and current from the PV array and the estimated frequency in Control Section A, Control Section B is able to regulate the output power of the PV plant. The implementation of the control is shown in Figure 4. Perturb and Observe (P&O) method is used to track the maximum power point (MPP) or the set point smaller than the MPP. Three modes of power generation are available: MPPT, unidirectional VSG and bidirectional VSG. In MPPT mode, the PV plant outputs as much power as possible and thus no bias power is added to the MPP, i.e. $\delta P^* = 0$. In the two VSG modes, a dynamic bias power is generated in response to the estimated frequency based on the swing equation of synchronous generator including damping effect, i.e. $\delta P^* = f(f, df/dt)$. The values of the virtual inertia J and the damping factor D determine the potency of the VSG control. Since the maximum power output is limited by the MPP, directly adding the VSG power bias to the MPP causes single sided action as the positive power bias is ineffective. In order to allow double sided power bias, a static power curtailment is necessary, leaving a controllable power margin to achieve bidirectional VSG, i.e. $\delta P^* = f(f, df/dt) - \Delta P$. The PV-VSG method actively compensates the power ramps caused by the PV and the loads, thereby reducing the use of battery. As we have mentioned before, the P&O method tracks the MPP as well as the new set point (MPP+δP^*) determined by the VSG, some modification has been made to the P&O. First, the tracked point is forced to the left slope of the power-voltage curve of the PV array because the left side is less sensitive to the change of voltage. Then the duty cycle accumulates according to the difference between the set point and

the measured value. However, unlike tracking the MPP where the slope goes to zero at the peak, tracking a set point on the left slope produces much more severe vibration. Therefore, a power-difference-dependent increment of duty cycle is applied to achieve fast tracking and high accuracy.

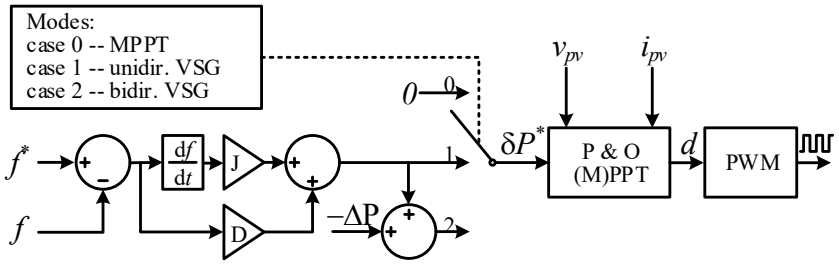

Figure 4: Implementation of Control Section B.

2.3. Control Section C

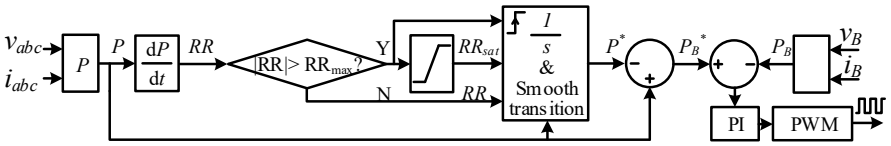

Figure 5: Implementation of Control Section C.

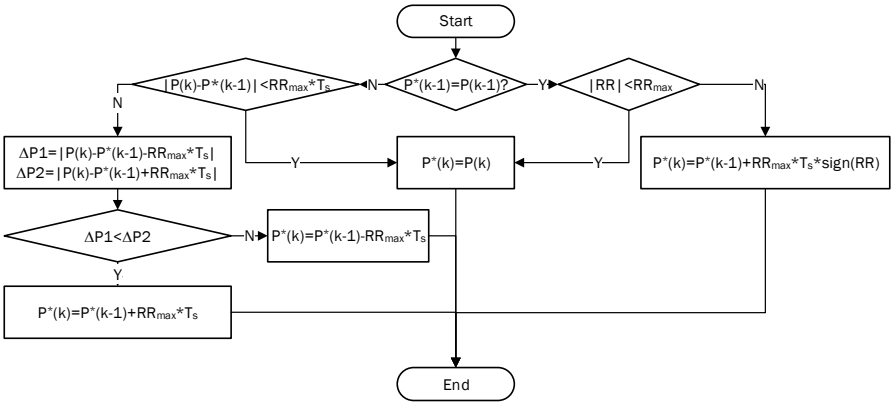

Figure 6: Generation of continuous desired power at the PCC with limited RR.

Control Section C controls the boost converter which joins the battery to the three phase inverter. With the measured voltage and current at the PCC, we can estimate the reference power for the BESS which limits the RR. The implementation of the control is shown in Figure 5. The power RR is calculated based on the obtained power at the PCC. If the RR exceeds the limit, it will be saturated to the limit; otherwise the RR is kept as it is. A desired power curve is then obtained based on the status of the actual power. In order to avoid discontinuity at desaturation, a smooth transition is necessary. The method of generating continuous RR-limited power curve at the PCC is described in the flowchart shown in Figure 6. If the desired output copies the input power in the previous state, it will follow the input as long as the RR stays

within the limit; otherwise the power will be regenerated based on the last tracked point and the maximum allowed RR, extending in the same direction as the input. If the output deviates from the input in the previous state, the proximity of the previous output to the current input will be checked to guarantee that it will not cause an over RR if we start to copy the input again. When the output is not allowed to copy the input, we need prolong the output curve by the maximum RR in a direction that minimizes the gap between the two curves.

Knowing the desired power curve at the PCC, the power reference for the battery system can be calculated and tracked by a PI regulated closed loop. Dead bind for the gap can be used in a way that balances the saving on batteries and the under-performance of the RR limitation.

3. Test Configuration and Results

The simulation is carried out using the system structure described in Figure 1 with a 250 kW salient-pole synchronous generator as the grid former, a 100 kW PV plant (under standard test condition) supported by a 2 kWh battery, and time-varying loads. The time step of the time-varying loads and irradiance is one minute. The 2-hour period at noon, between eleven and thirteen o'clock, is chosen to test the control strategy since both the average value and perturbation of the irradiance and the loads are significant. RRL methods generally require less installed capacity of batteries than RRS methods do, so the test results of the proposed method will be compared to that of a RRL method using only the battery in order to prove the improvement.

As expounded in the previous section, the power fluctuation at the PCC is first softened by the load compensation method which is automatically triggered by the estimated frequency and performed in Control Section A. Since this part is not RR tracking, we control the power flow at the battery side attempting to limit the RR under 10 kW/min in Control Section C. There are three options of how we regulate the output of the PV in Control Section B: the first case is to track the MPP; the second is to perform as a VSG only when the frequency goes up; the final one is to perform as a VSG responding to both rising and descending frequency ramps. Obviously, the second and the third cases sacrifice a portion of the PV generation to smooth the power spikes. However, since the VSG responds to the change of grid frequency, the excess power more than needed for RR limitation functions as ancillary service. Therefore, the estimation of the overall revenue should take three aspects into consideration: the loss in PV power supply, the savings on BESS and the remuneration for ancillary service, which needs further investigation into the electricity market. Therefore, the test is divided into two parts:

- Load Compensation with PV-MPPT
  In order prove that the proposed load compensation control can reduce the installed capacity of the battery, the test result is compared to that with only the battery limiting the RR.

- Load Compensation with PV-VSG by Power Curtailment
  As discussed before, even though the generation of the PV system is curtailed, there is possibility to compensate the economical loss by the savings on BESS and the provision of ancillary service. Therefore, the comparison among the results of the three PV power controls in Control Section B is made, focusing on the status of the battery and their auxiliary attainment of ancillary service.

3.1. Load Compensation with PV-MPPT

Figure 7 illustrates the test results from grid operational perspective. Figure 7(a) is the total power consumption of the non-inertial equipment at the PCC, i.e. the PV-BESS and the loads. Compared to the RRL by only the BESS (i.e. without load compensation), the proposed method succeeds in removing more high frequency dynamics due to the active load compensation. The overall RR at the PCC is shown in Figure 7(b). It limits the RR brought about by both the varying power generation and the varying loads. Figure 7(c) indicates the frequency profile of the microgrid. The proposed method improves the frequency transients because it has removed the power spikes applied to the grid former.

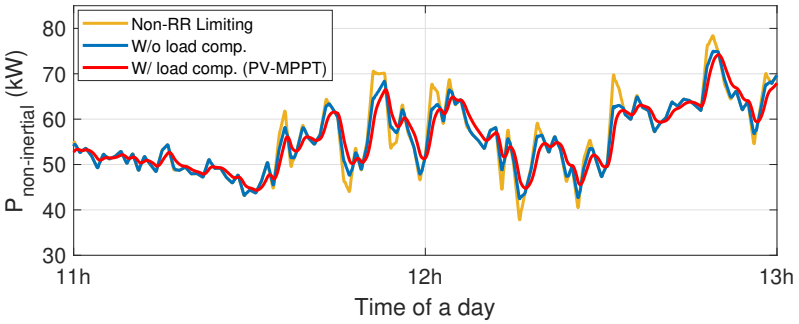

(a) Overall active power including time-varying generation and consumption

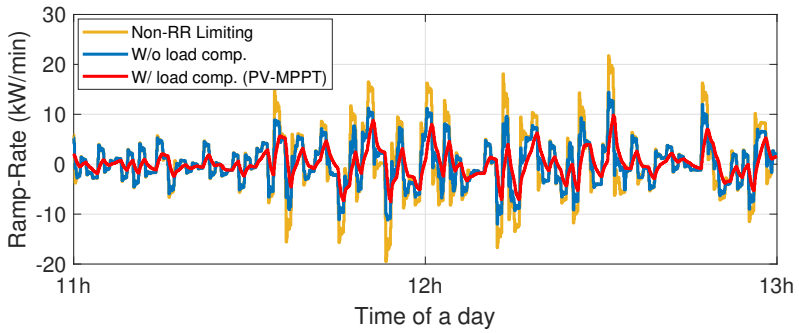

(b) Overall ramp-rate including time-varying generation and consumption

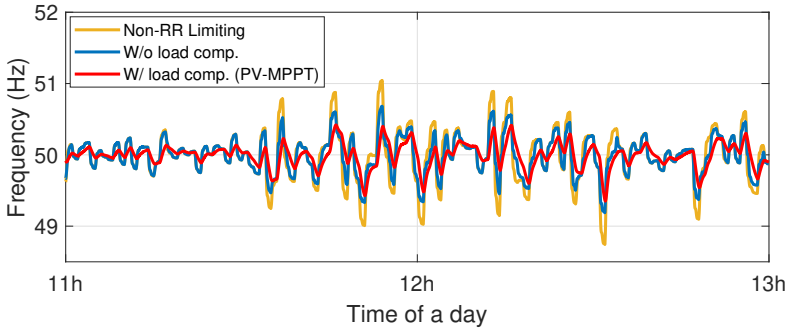

(c) Grid frequency

Figure 7: Grid profiles under non-RR limiting, RR limited by BESS without and with load compensation.

Figure 8 and Table 1 describe the power utilized in the BESS for RRL and the corresponding change of SoC between 11 h and 13 h. The initial SoC is set to 50 %. With the introduction of load compensation, the total depth of (dis)charge goes down (from 76.6 % to 19.6 %) and the number of (dis)charge cycles are reduced (from 31 to 13). The grey circles in Figure 8(b) mark the (dis)charge cycles eliminated by load compensation. The results indicate that the proposed method leads to a great reduction of the installed capacity and an improvement on the lifespan of the battery.

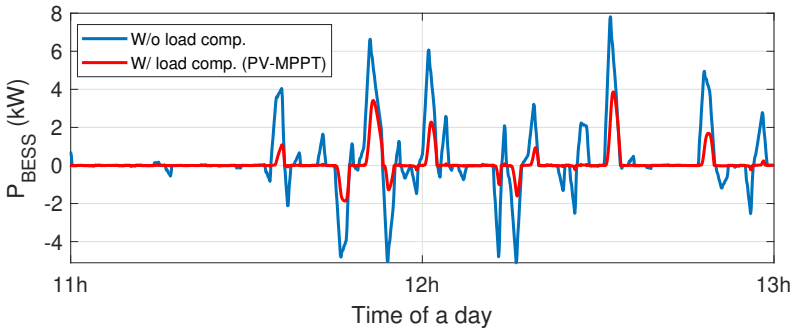

(a) Power generated / absorbed by the battery

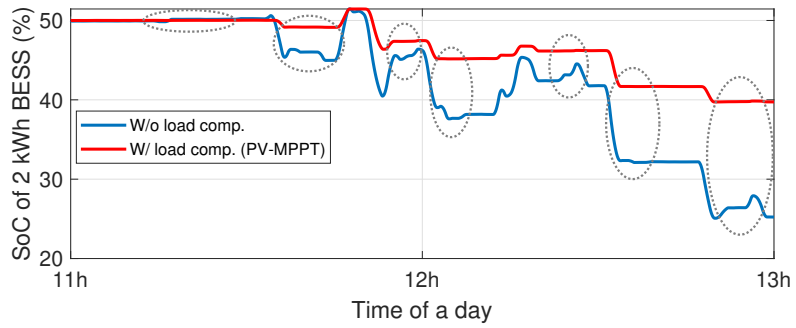

(b) SoC of the 2 kWh battery

Figure 8: Power and energy required from the BESS for RRL without and with load compensation.

Table 1: Use of battery (11-13 h) without and with load compensation under PV-MPPT control.

	Without load comp.	**With load comp.**
Tot. discharge	51.8 %	15.4 %
No. of discharge cycl.	15	7
Tot. charge	24.8 %	4.2 %
No. of charge cycl.	16	6

3.2. Load Compensation with PV-VSG by Power Curtailment

After demonstrating the improvement by load compensation, this section intends to discuss that how the curtailment of the PV power will further influence the performance on the basis of load compensation. The PV-VSG emulates the inertial behavior of synchronous machines in response to the frequency dynamics. The unidirectional PV-VSG conducts the duty by curtailing active power from the originally tracked MPP. The bidirectional PV-VSG, on the other hand, implements the task from a set point lower than the MPP.

The power contribution of the PV-BESS for the purpose of smoothing the power curve is drawn in Figure 9(a). The light and dark grey areas represent the power curtailment of the PV generation in bidirectional and unidirectional PV-VSG cases, respectively. The unidirectional PV-VSG compensates part of or all of the absorptive power demand from the BESS, but it is incapable of tackling the generative one. The bidirectional PV-VSG suppresses both absorptive and generative demands from the BESS but endures greater power loss because of the reserved power offset for bidirectional regulation. Consequently, the requirement for the battery changes because of the involvement of PV-VSG as depicted in Figure 9(a) by lines. This is also reflected in Figure 9(b) and Table 2. Compared to PV-MPPT, the unidirectional PV-VSG eliminates 3 charge cycles and brings down the charge energy from 4.2 % to 1.3 % in the test case. Therefore, its SoC curve avoids dramatic ramps up as circled by **A** and **B** in Figure 9(b). Even though the number of discharge cycles remains the same, the discharge energy slightly decreases. This is because the demanding power from the BESS is a result of system transients and the PV-VSG is a RRS control that may cause over limitation of the RR. In unidirectional PV-VSG case, the initial SoC can thus be set to a high value as the PV system undertakes the charge process together with the BESS. The bidirectional PV-VSG provides a complete power regulation on the basis of load compensation as long as the PV generation is no less than the need. Therefore, the two RRS controls (load compensation and bidirectional PV-VSG) concurrently soften the perturbative power curve before the BESS executes RRL, so the power provided by the battery is further reduced (from 19.6 % to 2.0 %) with fewer (dis)charge cycles (from 13 to 3). Therefore, a battery of smaller capacity can be applied to the RR control and its lifetime can be prolonged.

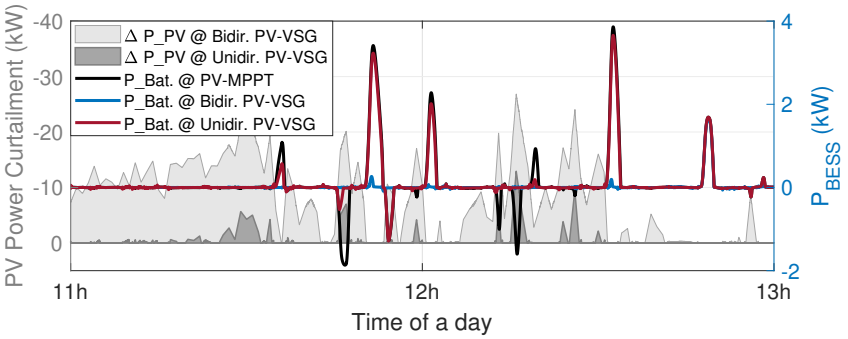

(a) Power profiles of the PV-BESS system

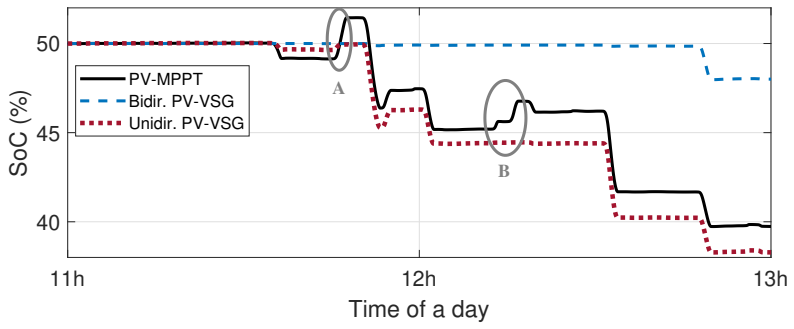

(b) SoC of the battery

Figure 9: PV-BESS under PV-MPPT and PV-VSG strategies.

The role of PV-VSG can be divided into two parts: to assist self-RR-mitigation and to conduct ancillary service. In severe cases where load compensation together with BESS RR limitation is insufficient to suppress the RR, PV-VSG will contribute to the self-RR-mitigation. Otherwise the PV-MPPT mode of the proposed method should cover the self-RR-mitigation duty as long as the battery is defined properly. So in such a

Table 2: Use of battery (11-13 h) with load compensation under different PV controls.

	PV-MPPT	**Unidir.PV-VSG**	**Bidir.PV-VSG**
Tot. discharge	15.4 %	13.2 %	2.0 %
No. of discharge cycl.	7	7	3
Tot. charge	4.2 %	1.3 %	0
No. of charge cycl.	6	3	0

case, the excess regulation due to PV-VSG further softens the power curve imposed on the grid former and thus improves the frequency dynamics and profits from providing ancillary service. The power curves at the PCC and the frequency dynamics are plotted in Figure 10 with the black colored curves under PV-MPPT mode being the reference. The red and blue areas in Figure 10(a) represent the removed stiffness from the reference power by unidirectional and bidirectional PV-VSG, respectively. Owing to the reserved power bias, the blue area fully covers the red one and is able to fill most power ramps that result in frequency transients. Even though the red area is less potent, it can fill part of steep power valleys. Reflecting in frequency, the unidirectional PV-VSG responds to over-frequency; the bidirectional PV-VSG deals with over- and under-frequency as indicated in Figure 10(b).

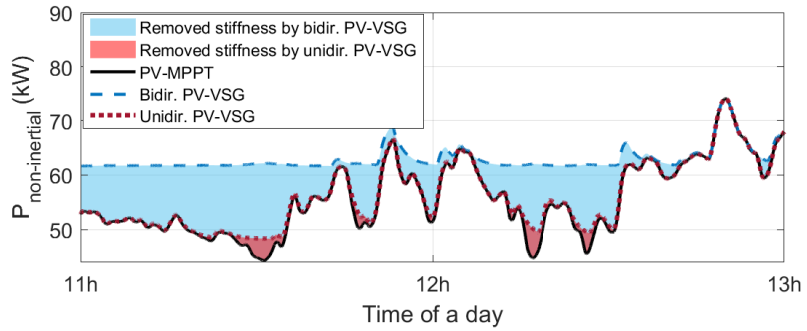

(a) Overall active power including time-varying generation and consumption

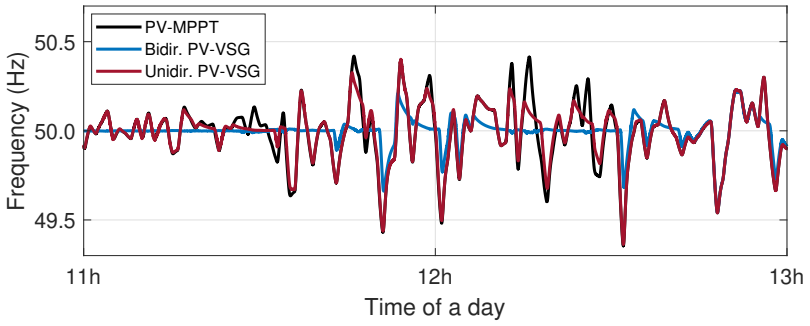

(b) Grid frequency

Figure 10: PV-VSG's contribution to ancillary service.

4. Conclusions

This paper proposed a novel control strategy to mitigate high ramp-rate in PV-integrated microgrids. Considering that time-varying loads have significant impact on grid frequency and their power consumption can be regulated to a certain extent in a network, the proposed control method counteracts the overall power ramps of the unpredictable PV generation and the fluctuating loads by the regulated load power consumption. Since the load compensation method performs RRS, the BESS attached to the PV system undertakes the duty to restrict the excessive RR to a preset boundary. Several simulations were performed on a microgrid system, demonstrating the effectiveness of the proposed control strategy in limiting the power RR and its advantage over relying on only the BESS to economize on batteries. Thereafter, three control modes of PV on the basis of load compensation were discussed with the aim of 1) assisting the load compensation method under extreme situations, 2) reducing the cost of the BESS and 3) providing ancillary service. The corresponding simulations showed that applying PV-VSG control succeeded in reducing the depth of (dis)charge and the number of (dis)charge cycles from a battery's perspective, and at the same time, made it possible to enhance the robustness of frequency from grid operational point of view.

References

References

[1] J. Rocabert, A. Luna, F. Blaabjerg, P. Rodríguez, Control of power converters in ac microgrids, IEEE Transactions on Power Electronics 27 (11) (2012) 4734–4749. doi:10.1109/TPEL.2012.2199334.

[2] S. D'Arco, J. A. Suul, O. B. Fosso, A virtual synchronous machine implementation for distributed control of power converters in smartgrids, Electric Power Systems Research 122 (2015) 180 – 197. doi:10.1016/j.epsr.2015.01.001.

[3] J. P. Lopes, N. Hatziargyriou, J. Mutale, P. Djapic, N. Jenkins, Integrating distributed generation into electric power systems: A review of drivers, challenges and opportunities, Electric Power Systems Research 77 (9) (2007) 1189 – 1203, distributed Generation. doi:10.1016/j.epsr.2006.08.016.

[4] Y. Huo, G. Gruosso, Hardware-in-the-loop framework for validation of ancillary service in microgrids: Feasibility, problems and improvement, IEEE Access 7 (2019) 58104–58112. doi:10.1109/ACCESS.2019.2914346.

[5] V. Gevorgian, S. Booth, Review of prepa technical requirements for interconnecting wind and solar generation, Tech. rep., National Renewable Energy Lab.(NREL), Golden, CO (United States) (2013).

[6] F. Fattori, N. Anglani, I. Staffell, S. Pfenninger, High solar photovoltaic penetration in the absence of substantial wind capacity: Storage requirements and effects on capacity adequacy, Energy 137 (2017) 193 – 208. doi:https://doi.org/10.1016/j.energy.2017.07.007.
URL http://www.sciencedirect.com/science/article/pii/S0360544217311817

[7] R. V. Haaren, M. Morjaria, V. Fthenakis, An energy storage algorithm for ramp rate control of utility scale pv (photovoltaics) plants, Energy 91 (2015) 894 – 902. doi:https://doi.org/10.1016/j.energy.2015.08.081.
URL http://www.sciencedirect.com/science/article/pii/S0360544215011573

[8] N. Miller, D. Manz, J. Roedel, P. Marken, E. Kronbeck, Utility scale battery energy storage systems, in: IEEE PES General Meeting, 2010, pp. 1–7. doi:10.1109/PES.2010.5589871.

[9] C. A. Hill, M. C. Such, D. Chen, J. Gonzalez, W. M. Grady, Battery energy storage for enabling integration of distributed solar power generation, IEEE Transactions on Smart Grid 3 (2) (2012) 850–857. doi:10.1109/TSG.2012.2190113.

[10] H. Beltran, I. Tomás García, J. C. Alfonso-Gil, E. Pérez, Levelized cost of storage for li-ion batteries used in pv power plants for ramp-rate control, IEEE Trans. Energy Convers. 34 (1) (2019) 554–561. doi:10.1109/TEC.2019.2891851.

[11] J. Marcos, O. Storkël, L. Marroyo, M. Garcia, E. Lorenzo, Storage requirements for pv power ramp-rate control, Solar Energy 99 (2014) 28 – 35. doi:https://doi.org/10.1016/j.solener.2013.10.037.
URL http://www.sciencedirect.com/science/article/pii/S0038092X13004672

[12] A. Makibar, L. Narvarte, E. Lorenzo, On the relation between battery size and pv power ramp rate limitation, Solar Energy 142 (2017) 182 – 193. doi:https://doi.org/10.1016/j.solener.2016.11.039.
URL http://www.sciencedirect.com/science/article/pii/S0038092X16305795

[13] S. Pourmousavi, T. K. Saha, Evaluation of the battery operation in ramp-rate control mode within a pv plant: A case study, Solar Energy 166 (2018) 242 – 254. doi:https://doi.org/10.1016/j.solener.2018.03.035.
URL http://www.sciencedirect.com/science/article/pii/S0038092X18302482

[14] S. Sukumar, M. Marsadek, K. Agileswari, H. Mokhlis, Ramp-rate control smoothing methods to control output power fluctuations from solar photovoltaic (pv) sources—a review, J. Energy Storage 20 (2018) 218 – 229. doi:https://doi.org/10.1016/j.est.2018.09.013.
URL http://www.sciencedirect.com/science/article/pii/S2352152X18302366

[15] X. Chen, Y. Du, H. Wen, L. Jiang, W. Xiao, Forecasting-based power ramp-rate control strategies for utility-scale pv systems, IEEE Trans. Ind. Electron. 66 (3) (2019) 1862–1871. doi:10.1109/TIE.2018.2840490.

[16] X. Ai, J. Li, J. Fang, W. Yao, H. Xie, R. Cai, J. Wen, Multi-time-scale coordinated ramp-rate control for photovoltaic plants and battery energy storage, IET Renew. Power Gener. 12 (12) (2018) 1390–1397. doi:10.1049/iet-rpg.2018.5190.

[17] I. de la Parra, J. Marcos, M. García, L. Marroyo, Control strategies to use the minimum energy storage requirement for pv power ramp-rate control, Solar Energy 111 (2015) 332 – 343. doi:https://doi.org/10.1016/j.solener.2014.10.038.
URL http://www.sciencedirect.com/science/article/pii/S0038092X14005258

[18] S. B. Y. Liu, L. J. Garces, System and method for controlling ramp rate of solar photovoltaic system (12 2014).
URL https://patentimages.storage.googleapis.com/9f/25/a0/57b9d9f8a2834c/US8901411.pdf

[19] D. Lamsal, V. Sreeram, Y. Mishra, D. Kumar, Smoothing control strategy of wind and photovoltaic output power fluctuation by considering the state of health of battery energy storage system, IET Renew. Power Gen. 13 (4) (2019) 578–586. doi:10.1049/iet-rpg.2018.5111.

[20] M. Datta, T. Senjyu, A. Yona, T. Funabashi, C.-H. Kim, Photovoltaic output power fluctuations smoothing methods for single and multiple pv generators, Curr. Appl. Phys. 10 (2, Supplement) (2010) S265 – S270, the Proceeding of the International Renewable Energy Conference and Exhibition 2008 (RE2008). doi:https://doi.org/10.1016/j.cap.2009.11.027.
URL http://www.sciencedirect.com/science/article/pii/S1567173909005239

[21] M. Datta, T. Senjyu, Fuzzy control of distributed pv inverters/energy storage systems/electric vehicles for frequency regulation in a large power system, IEEE Trans. Smart Grid 4 (1) (2013) 479–488. doi:10.1109/TSG.2012.2237044.

[22] X. Li, Y. Li, X. Han, D. Hui, Application of fuzzy wavelet transform to smooth wind/pv hybrid power system output with battery energy storage system, Energy Procedia 12 (2011) 994 – 1001. doi:https://doi.org/10.1016/j.egypro.2011.10.130.
URL http://www.sciencedirect.com/science/article/pii/S1876610211019564

[23] X. Li, D. Hui, X. Lai, Battery energy storage station (bess)-based smoothing control of photovoltaic (pv) and wind power generation fluctuations, IEEE Trans. Sustainable Enery 4 (2) (2013) 464–473. doi:10.1109/TSTE.2013.2247428.

[24] J.-L. Duchaud, G. Notton, C. Darras, C. Voyant, Power ramp-rate control algorithm with optimal state of charge reference via dynamic programming, Energy 149 (2018) 709 – 717. doi:https://doi.org/10.1016/j.energy.2018.02.064.
URL http://www.sciencedirect.com/science/article/pii/S0360544218302925

[25] M. J. E. Alam, K. M. Muttaqi, D. Sutanto, A novel approach for ramp-rate control of solar pv using energy storage to mitigate output fluctuations caused by cloud passing, IEEE Trans. Energy Convers. 29 (2) (2014) 507–518. doi:10.1109/TEC.2014.2304951.

[26] W. A. Omran, M. Kazerani, M. M. A. Salama, Investigation of methods for reduction of power fluctuations generated from large grid-connected photovoltaic systems, IEEE Trans. Energy Convers. 26 (1) (2011) 318–327. doi:10.1109/TEC.2010.2062515.

[27] S. Barcellona, Y. Huo, R. Niu, L. Piegari, E. Ragaini, Control strategy of virtual synchronous generator based on virtual impedance and band-pass damping, in: 2016 International Symposium on Power Electronics, Electrical Drives, Automation and Motion (SPEEDAM), 2016, pp. 1354–1362. doi:10.1109/SPEEDAM.2016.7525999.